

Evaluation of neutron tagging efficiency on 0.03% Gd mass concentration in SK-Gd experiment

Fumi Nakanishi^{a,*} and for the Super-Kamiokande Collaboration

^aOkayama University,

Okayama-shi, Okayama, 700-8530, Japan

E-mail: nakanishi-suv@s.okayama-u.ac.jp

Super-Kamiokande (SK) experiment started the "SK-Gd experiment" by dissolving gadolinium (Gd) sulfate octa-hydrate in ultra-pure water from the tank in July 2020. The neutron tagging efficiency has been improved compared to the pure-water phase by detecting a total energy of 8 MeV gamma rays emitted by thermal neutron capture on Gd. It enables us to improve, for example, the sensitivity of diffuse supernova neutrino background, the accuracy of the reconstruction for the supernova direction, and so on. For these physics targets, accurate evaluation of neutron identification efficiency is essential. In this presentation, I report the calibration results using an Am/Be neutron source to evaluate the efficiency at a Gd mass concentration of 0.03%, starting from June 2022, and the comparison of the estimated neutron detection efficiency with simulation.

38th International Cosmic Ray Conference (ICRC2023)
26 July - 3 August, 2023
Nagoya, Japan



*Speaker

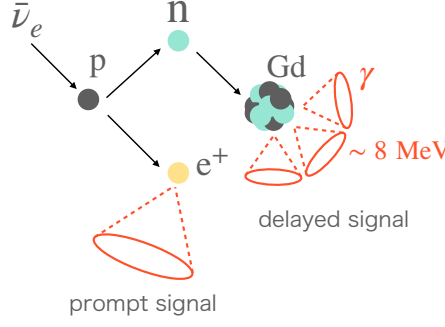


Figure 1: Idea of the delayed coincidence method for identification of inverse beta decay (IBD) in SK-Gd.

1. Introduction

Detecting neutrons is crucial for the Super-Kamiokande (SK) experiment[1], to improve many kinds of physics sensitivity. However, since the major neutron signal in the pure-water detector is 2.2 MeV gamma-ray from neutron capture on a proton, the neutron tagging efficiency using this gamma-ray is only about 20% due to its low energy for SK.

To improve neutron tagging efficiency, in 2020, SK dissolved 13 tons of gadolinium sulfate octahydrate to its 50 kilotons of ultra-pure water[2]. This marked the beginning of a new phase, SK-Gd (SK-VI). The total energy of multiple gamma-rays from thermal neutron capture on Gd is about 8 MeV. This higher energy makes it possible to identify the neutron capture reaction more effectively. Figure 1 shows the basic idea of the delayed coincidence method, which uses a prompt positron signal and a delayed neutron signal[3]. By dissolving about 0.01% of the Gd in mass concentration, roughly 50% of neutrons is captured on Gd nuclei. In previous study[4], the tagging efficiency without materials relevant to our source is estimated to be 40.5 ± 0.1 (stat.) $^{+1.0}_{-2.1}$ (sys.)%.

In 2022, SK dissolved additional 26 tons of gadolinium sulfate octahydrate, and a new phase of the SK-Gd experiment was started (SK-VII). With this improvement, the mass concentration of Gd increased to about 0.03%, and roughly 75% of neutrons will be captured on Gd nuclei as shown in Figure 2.

2. Am/Be source measurement

Evaluation of the neutron tagging efficiency is essential to estimate physics sensitivity in SK-Gd. Therefore, we studied neutron detection using an Americium-241/Beryllium-9 (Am/Be) radioactive source. Am/Be source is famous for its neutron emission accompanying gamma-ray. The main reaction chain can be described as $^{241}\text{Am} \rightarrow ^{237}\text{Np} + \alpha$, $^9\text{Be} + \alpha \rightarrow ^{12}\text{C} + n + \gamma(4.4 \text{ MeV})$. This measurement uses a prompt 4.4 MeV gamma-ray and a delayed neutron as the target of the delayed coincidence.

For separating 4.4 MeV gamma-ray from other low energy events, we installed the source with the BGO scintillator crystal to enhance gamma-ray light yield. In the previous study on SK-VI ([4]), to estimate the unexpected effect of BGO crystal on the tagging efficiency, two kinds of source configure, which are "1 BGO" and "8 BGO", were used. While the 8 BGO structure is that source is fully surrounded by eight BGO crystals, the structure of the 1 BGO configure is that source is

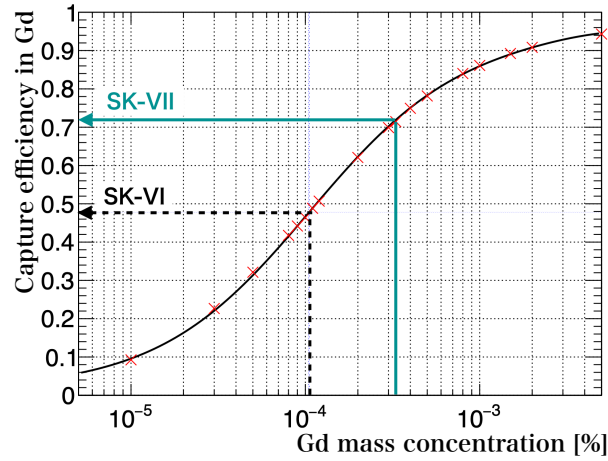


Figure 2: The relationship between Gd mass concentration and capture efficiency in Gd. The capture efficiency increased about 1.5 times from SK-VI to SK-VII.

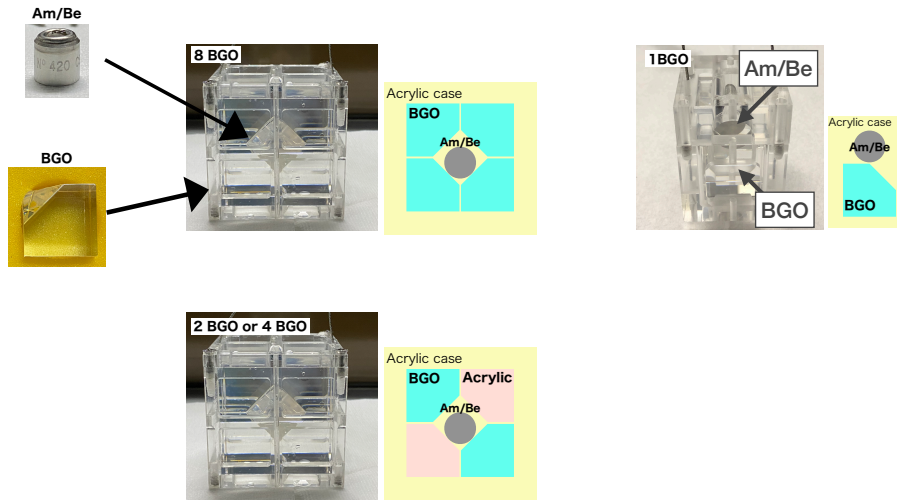


Figure 3: Appearance of the source set up for 8 BGO, 1 BGO (upper), and 2 or 4 BGO structure (lower).

installed with one BGO. In this study, we measured newly two kinds of source configure, which are "2 BGO" and "4 BGO". These new structures are the same as 8 BGO structures but not fully surrounded by eight crystals, but a portion of the BGO is replaced with acrylic. The picture of Am/Be source and BGO crystals are shown in Figure 3

3. Analysis

The neutron tagging efficiency ϵ_n is evaluated by this formula:

$$\epsilon_n = \frac{(\text{Number of tagged neutrons}) - (\text{Number of estimated background})}{(\text{Number of prompt events})} \quad (1)$$

For selecting a prompt event induced by our Am/Be + BGO source, the total photo-electrons measured by PMTs for the inner detector (ID) is used. Figure 4 shows the total observed photo-electrons distribution of the events. The events with its photo-electrons are around 1000 p.e. are

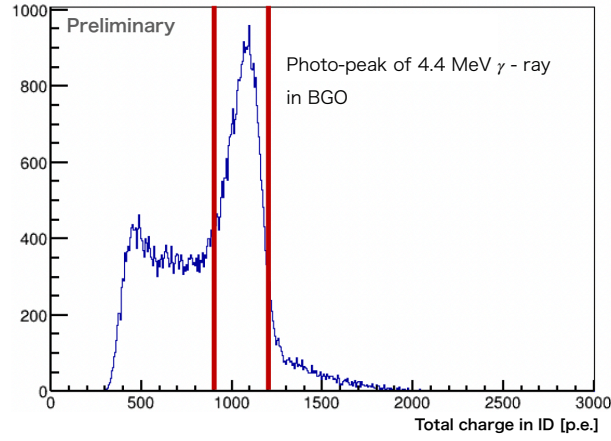


Figure 4: Distribution of the total photo-electrons measured by PMTs for the inner detector. The peak which is seen around 1000 p.e. represents the photo peak of the 4.4 MeV gamma-ray on the BGO scintillator.

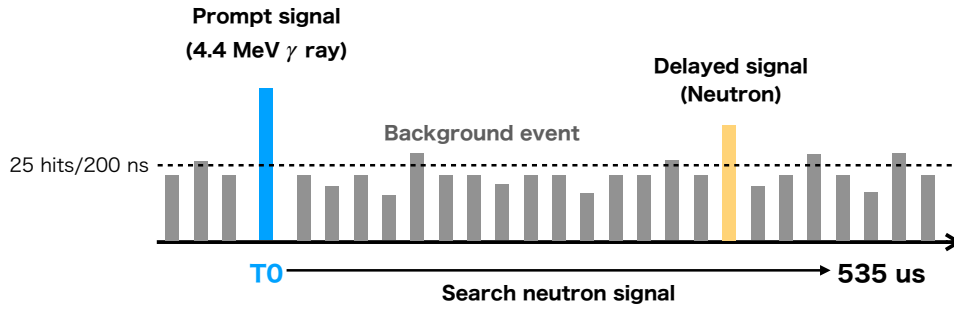


Figure 5: Schematic diagram of data acquisition structure.

selected as the prompt event for all the following analyses. All hits within $535 \mu\text{s}$ after these events are recorded and analyzed for delayed neutron search. Delayed neutron signals are searched in the time range between $4 \mu\text{s}$ and $535 \mu\text{s}$ after the prompt event. Figure 5 is the schematic diagram of data acquisition structure. By scanning with a 200 ns time window, the hit cluster with more than 25 hits are selected as a neutron candidate. Neutron signals are classified using five cut criteria about event reconstruction for each candidate. Figure 6 shows two of the five cut variable's distribution and criteria. Filled histograms show the neutron signal computed by the Monte-Carlo simulation (MC). A fiducial volume cut which removes events within the 2 m from the tank wall, is already applied. In this study, we used background data of 0.01% Gd mass concentration phase in MC simulation, because the background estimation of 0.03% Gd mass concentration has not completed yet. However, this discrepancy has little effect in calculating neutron tagging efficiency because the signal components are almost comparable in data and MC.

4. Result

The distribution of the time difference between the prompt event and the delayed event of tagged neutron is shown in Figure 7. The time constant τ was obtained by fitting this distribution,

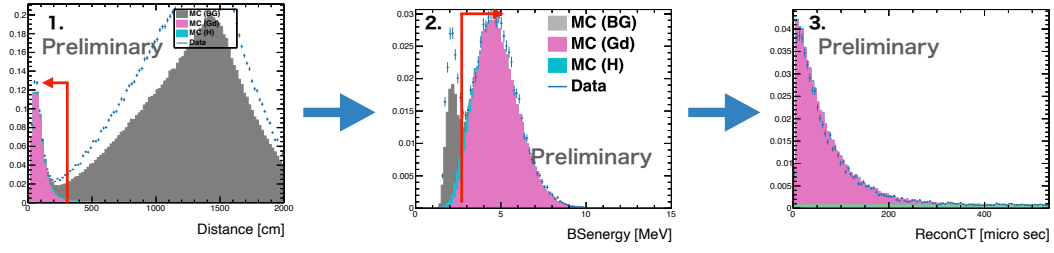


Figure 6: Distributions of the cut variables. 1. Distance from the source, and 2. Reconstructed energy. After all cuts, we can obtain the time difference distribution from the prompt event of neutron event in 3. The red arrows show the cut criteria. These plots already applied the cut of former number.

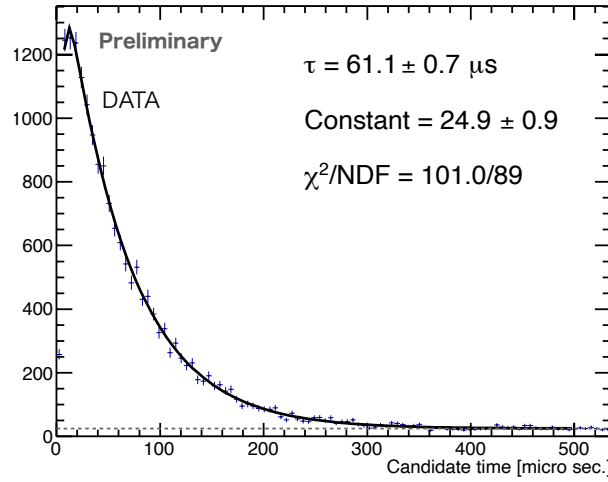


Figure 7: Time difference distribution from the prompt event of neutron event of detector center (8 BGO).

and the result is almost consistent with the expected value (about $61 \mu\text{s}$). The number of background candidates is evaluated from the same fit of timing distribution.

The correlation between the tagging efficiency and the number of surrounding BGO is evaluated by the data at the detector center as shown in Figure 8. The value obtained by data tends to be smaller than MC estimation. The relative difference is 5.2%(5.9%) in the case of 1 BGO (8 BGO). We concluded that the remaining $\sim 5\%$ of discrepancy inevitably comes from the unknown effect of BGO and the detailed difference in data structure between actual data and MC. Our systematic error estimation includes the uncertainty of Am/Be source properties, MC conditions, the cut criteria, and dependence on the source position. Tagging efficiency depends on the number of BGOs, which is lower if there are many BGOs. The neutron tagging efficiency without any BGO is estimated to be $59.7 \pm 1.2(\text{stat.} + \text{sys.})\%$ by MC simulation. The probability of a misidentification noise event is 0.33%, which is a bit larger than the 0.01% Gd concentration phase due to increasing dark noise.

We measured at 15 positions to estimate position uniformity of tagging efficiency and time difference on September 2022. Figure 9 and Figure 10 show the position uniformity of tagging efficiency and time difference from the prompt event of neutron event, respectively. The values at each position are in agreement within the statistical error in both tagging efficiency and time difference. We estimated the weighted mean of tagging efficiency and time difference, $51.68 \pm 0.13\%$

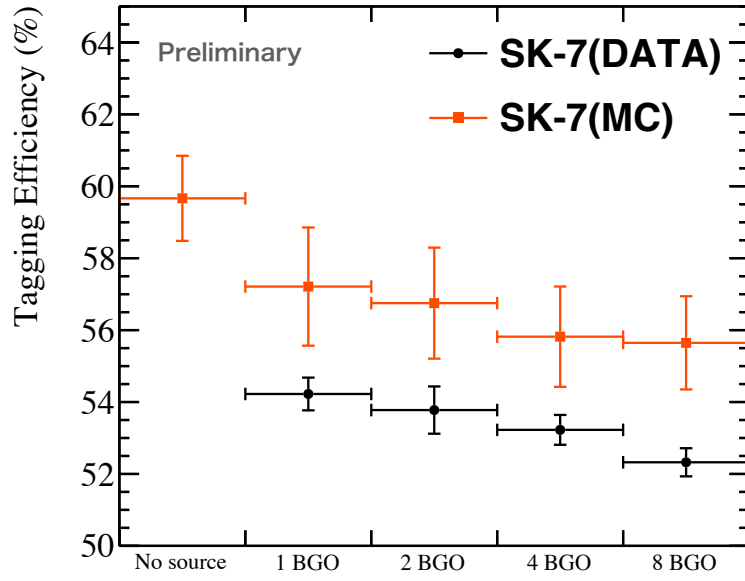


Figure 8: The tagging efficiency for each BGO. The black circles show data, and red squares show MC. The error of MC includes statistical and systematic errors.

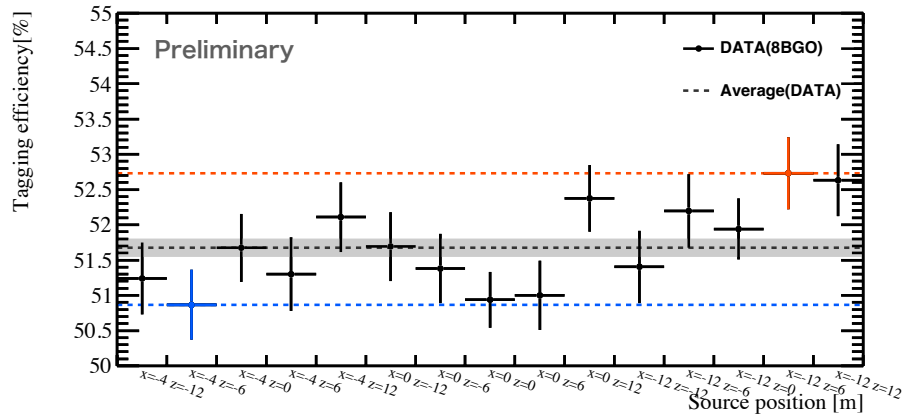


Figure 9: The position uniformity of the tagging efficiency. The maximum value is 52.73% shown as red, and the minimum value is 50.87% shown as blue.

and $61.56 \pm 0.18 \mu s$.

5. Conclusion

We evaluated the tagging efficiency in a new phase of SK-Gd with an increased Gd mass concentration of 0.03%. As a result, the efficiency without materials relevant to our source is estimated to be 59.7 ± 1.2 (stat. + sys.)% by MC simulation, and that increase 1.47 times compared with the 0.01% Gd concentration phase. We confirmed that the results are comparable with expectations. The remaining difference between data and MC comes from evaluating background candidates and understanding BGO characteristics.

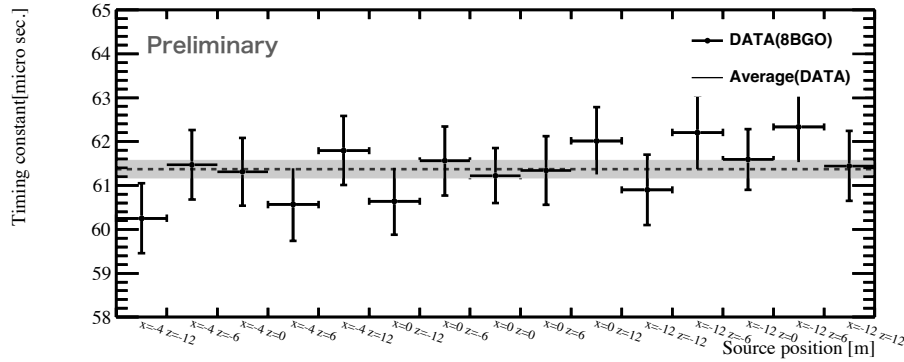


Figure 10: The position uniformity of the time difference from prompt event of neutron event.

We estimated position uniformity of tagging efficiency and time difference from the prompt event of neutron event. We can confirm that they are stable within the statistical error.

As future prospects, we are approaching the MC improvement for 0.03% Gd mass concentration phase, and we will re-estimate neutron tagging efficiency and systematic uncertainty using noise data of 0.03% Gd mass concentration phase after final tuning in MC.

References

- [1] S. Fukuda, Y. Fukuda, T. Hayakawa, E. Ichihara, M. Ishitsuka, Y. Itow et al., *The super-kamiokande detector*, *Nuclear Instruments and Methods in Physics Research Section A: Accelerators, Spectrometers, Detectors and Associated Equipment* **501** (2003) 418.
- [2] K. Abe, C. Bronner, Y. Hayato, K. Hiraide, M. Ikeda, S. Imaizumi et al., *First gadolinium loading to super-kamiokande*, *Nuclear Instruments and Methods in Physics Research Section A: Accelerators, Spectrometers, Detectors and Associated Equipment* **1027** (2022) 166248.
- [3] J.F. Beacom and M.R. Vagins, *Antineutrino spectroscopy with large water Čerenkov detectors*, *Phys. Rev. Lett.* **93** (2004) 171101.
- [4] M. Harada, *Evaluation of neutron tagging efficiency for SK-Gd experiment*, in *Proceedings of 41st International Conference on High Energy physics — PoS(ICHEP2022)*, vol. 414, p. 1178, 2022, DOI.

Full Authors List: Collaboration

K. Abe^{1,46}, C. Bronner¹, Y. Hayato^{1,46}, K. Hiraide^{1,46}, K. Hosokawa¹, K. Ieki^{1,46}, M. Ikeda^{1,46}, J. Kameda^{1,46}, Y. Kanemura¹, R. Kaneshima¹, Y. Kashiwagi¹, Y. Kataoka^{1,46}, S. Miki¹, S. Mine^{1,6}, M. Miura^{1,46}, S. Moriyama^{1,46}, Y. Nakano¹, M. Nakahata^{1,46}, S. Nakayama^{1,46}, Y. Noguchi¹, K. Sato¹, H. Sekiya^{1,46}, H. Shiba¹, K. Shimizu¹, M. Shiozawa^{1,46}, Y. Sonoda¹, Y. Suzuki¹, A. Takeda^{1,46}, Y. Takemoto^{1,46}, H. Tanaka^{1,46}, T. Yano¹, S. Han², T. Kajita^{2,46,22}, K. Okumura^{2,46}, T. Tashiro², T. Tomiya², X. Wang², S. Yoshida², P. Fernandez³, L. Labarga³, N. Ospina³, B. Zaldivar³, B. W. Pointon^{5,49}, E. Kearns^{4,46}, J. L. Raaf⁴, L. Wan⁴, T. Wester⁴, J. Bian⁶, N. J. Griskevich⁶, S. Locke⁶, M. B. Smy^{6,46}, H. W. Sobel^{6,46}, V. Takhistov^{6,24}, A. Yankelevich⁶, J. Hill⁷, S. H. Lee⁸, D. H. Moon⁸, R. G. Park⁸, B. Bodur⁹, K. Scholberg^{9,46}, C. W. Walter^{9,46}, A. Beauchêne¹⁰, O. Drapier¹⁰, A. Giampaolo¹⁰, Th. A. Mueller¹⁰, A. D. Santos¹⁰, P. Paganini¹⁰, B. Quilain¹⁰, T. Nakamura¹¹, J. S. Jang¹², L. N. Machado¹³, J. G. Learned¹⁴, K. Choi¹⁵, N. Iovine¹⁵, S. Cao¹⁶, L. H. V. Anthony¹⁷, D. Martin¹⁷, N. W. Prouse¹⁷, M. Scott¹⁷, A. A. Sztuc¹⁷, Y. Uchida¹⁷, V. Berardi¹⁸, M. G. Catanesi¹⁸, E. Radicioni¹⁸, N. F. Calabria¹⁹, A. Langella¹⁹, G. De Rosa¹⁹, G. Collazuol²⁰, F. Iacob²⁰, M. Mattiuzzi²⁰, L. Ludovici²¹, M. Gonin²², G. Pronost²², C. Fujisawa²³, Y. Maekawa²³, Y. Nishimura²³, R. Okazaki²³, R. Akutsu²⁴, M. Friend²⁴, T. Hasegawa²⁴, T. Ishida²⁴, T. Kobayashi²⁴, M. Jakkapu²⁴, T. Matsubara²⁴, T. Nakadaira²⁴, K. Nakamura^{24,46}, Y. Oyama²⁴, K. Sakashita²⁴, T. Sekiguchi²⁴, T. Tsukamoto²⁴, N. Bhuiyan²⁵, G. T. Burton²⁵, F. Di Lodovico²⁵, J. Gao²⁵, A. Goldsack²⁵, T. Katori²⁵, J. Migenda²⁵, Z. Xie²⁵, S. Szoldos^{25,46}, A. T. Suzuki²⁶, Y. Takagi²⁶, Y. Takeuchi^{26,46}, J. Feng²⁷, L. Feng²⁷, J. R. Hu²⁷, Z. Hu²⁷, T. Kikawa²⁷, M. Mori²⁷, T. Nakaya^{27,46}, R. A. Wendell^{27,46}, K. Yasutome²⁷, S. J. Jenkins²⁸, N. McCauley²⁸, P. Mehta²⁸, A. Tarant²⁸, Y. Fukuda²⁹, Y. Itow^{30,31}, H. Menjo³⁰, K. Ninomiya³⁰, J. Lagoda³², S. M. Lakshmi³², M. Mandal³², P. Mijakowski³², Y. S. Prabhu³², J. Zalipska³², M. Jia³³, J. Jiang³³, C. K. Jung³³, M. J. Wilking³³, C. Yanagisawa^{33,†}, M. Harada³⁴, Y. Hino³⁴, H. Ishino³⁴, Y. Koshio^{34,46}, F. Nakanishi³⁴, S. Sakai³⁴, T. Tada³⁴, T. Tano³⁴, T. Ishizuka³⁵, G. Barr³⁶, D. Barrow³⁶, L. Cook^{36,46}, S. Samani³⁶, D. Wark^{36,41}, A. Holin³⁷, F. Nova³⁷, B. S. Yang³⁸, J. Y. Yang³⁸, J. Yoo³⁸, J. E. P. Fannon³⁹, L. Kneale³⁹, M. Malek³⁹, J. M. McElwee³⁹, M. D. Thiesse³⁹, L. F. Thompson³⁹, S. T. Wilson³⁹, H. Okazawa⁴⁰, S. B. Kim⁴², E. Kwon⁴², J. W. Seo⁴², I. Yu⁴², A. K. Ichikawa⁴³, K. D. Nakamura⁴³, S. Tairafune⁴³, K. Nishijima⁴⁴, A. Eguchi⁴⁵, K. Nakagiri⁴⁵, Y. Nakajima^{45,46}, S. Shima⁴⁵, N. Taniuchi⁴⁵, E. Watanabe⁴⁵, M. Yokoyama^{45,46}, P. de Perio⁴⁶, S. Fujita⁴⁶, K. Martens⁴⁶, K. M. Tsui⁴⁶, M. R. Vagins^{46,6}, J. Xia⁴⁶, S. Izumiya⁴⁷, M. Kuze⁴⁷, R. Matsumoto⁴⁷, M. Ishitsuka⁴⁸, H. Ito⁴⁸, Y. Ommura⁴⁸, N. Shigeta⁴⁸, M. Shinoki⁴⁸, K. Yamauchi⁴⁸, T. Yoshida⁴⁸, R. Gaur⁴⁹, V. Gousy-Leblanc^{49,‡}, M. Hartz⁴⁹, A. Konaka⁴⁹, X. Li⁴⁹, S. Chen⁵⁰, B. D. Xu⁵⁰, B. Zhang⁵⁰, M. Posiadala-Zezula⁵¹, S. B. Boyd⁵², R. Edwards⁵², D. Hadley⁵², M. Nicholson⁵², M. O'Flaherty⁵², B. Richards⁵², A. Ali^{53,49}, B. Jamieson⁵³, S. Amanai⁵⁴, Ll. Marti⁵⁴, A. Minamino⁵⁴, and S. Suzuki⁵⁴

¹Kamioka Observatory, Institute for Cosmic Ray Research, University of Tokyo, Kamioka, Gifu 506-1205, Japan²Research Center for Cosmic Neutrinos, Institute for Cosmic Ray Research, University of Tokyo, Kashiwa, Chiba 277-8582, Japan³Department of Theoretical Physics, University Autonoma Madrid, 28049 Madrid, Spain⁴Department of Physics, Boston University, Boston, MA 02215, USA⁵Department of Physics, British Columbia Institute of Technology, Burnaby, BC, V5G 3H2, Canada⁶Department of Physics and Astronomy, University of California, Irvine, Irvine, CA 92697-4575, USA⁷Department of Physics, California State University, Dominguez Hills, Carson, CA 90747, USA⁸Institute for Universe and Elementary Particles, Chonnam National University, Gwangju 61186, Korea⁹Department of Physics, Duke University, Durham NC 27708, USA¹⁰Ecole Polytechnique, IN2P3-CNRS, Laboratoire Leprince-Ringuet, F-91120 Palaiseau, France¹¹Department of Physics, Gifu University, Gifu, Gifu 501-1193, Japan¹²GIST College, Gwangju Institute of Science and Technology, Gwangju 500-712, Korea¹³School of Physics and Astronomy, University of Glasgow, Glasgow, Scotland, G12 8QQ, United Kingdom¹⁴Department of Physics and Astronomy, University of Hawaii, Honolulu, HI 96822, USA¹⁵Institute for Basic Science (IBS), Daejeon, 34126, Korea¹⁶Institute For Interdisciplinary Research in Science and Education, ICISE, Quy Nhon, 55121, Vietnam¹⁷Department of Physics, Imperial College London, London, SW7 2AZ, United Kingdom¹⁸Dipartimento Interuniversitario di Fisica, INFN Sezione di Bari and Università e Politecnico di Bari, I-70125, Bari, Italy¹⁹Dipartimento di Fisica, INFN Sezione di Napoli and Università di Napoli, I-80126, Napoli, Italy²⁰Dipartimento di Fisica, INFN Sezione di Padova and Università di Padova, I-35131, Padova, Italy²¹INFN Sezione di Roma and Università di Roma "La Sapienza", I-00185, Roma, Italy²²ILANCE, CNRS - University of Tokyo International Research Laboratory, Kashiwa, Chiba 277-8582, Japan²³Department of Physics, Keio University, Yokohama, Kanagawa, 223-8522, Japan²⁴High Energy Accelerator Research Organization (KEK), Tsukuba, Ibaraki 305-0801, Japan²⁵Department of Physics, King's College London, London, WC2R 2LS, UK²⁶Department of Physics, Kobe University, Kobe, Hyogo 657-8501, Japan²⁷Department of Physics, Kyoto University, Kyoto, Kyoto 606-8502, Japan²⁸Department of Physics, University of Liverpool, Liverpool, L69 7ZE, United Kingdom²⁹Department of Physics, Miyagi University of Education, Sendai, Miyagi 980-0845, Japan³⁰Institute for Space-Earth Environmental Research, Nagoya University, Nagoya, Aichi 464-8602, Japan³¹Kobayashi-Maskawa Institute for the Origin of Particles and the Universe, Nagoya University, Nagoya, Aichi 464-8602, Japan³²National Centre For Nuclear Research, 02-093 Warsaw, Poland³³Department of Physics and Astronomy, State University of New York at Stony Brook, NY 11794-3800, USA³⁴Department of Physics, Okayama University, Okayama, Okayama 700-8530, Japan³⁵Media Communication Center, Osaka Electro-Communication University, Neyagawa, Osaka, 572-8530, Japan³⁶Department of Physics, Oxford University, Oxford, OX1 3PU, United Kingdom³⁷Rutherford Appleton Laboratory, Harwell, Oxford, OX11 0QX, UK³⁸Department of Physics, Seoul National University, Seoul 151-742, Korea[†]also at BMCC/CUNY, Science Department, New York, New York, 1007, USA.[‡]also at University of Victoria, Department of Physics and Astronomy, PO Box 1700 STN CSC, Victoria, BC V8W 2Y2, Canada.

- ³⁹Department of Physics and Astronomy, University of Sheffield, S3 7RH, Sheffield, United Kingdom
⁴⁰Department of Informatics in Social Welfare, Shizuoka University of Welfare, Yaizu, Shizuoka, 425-8611, Japan
⁴¹STFC, Rutherford Appleton Laboratory, Harwell Oxford, and Daresbury Laboratory, Warrington, OX11 0QX, United Kingdom
⁴²Department of Physics, Sungkyunkwan University, Suwon 440-746, Korea
⁴³Department of Physics, Faculty of Science, Tohoku University, Sendai, Miyagi, 980-8578, Japan
⁴⁴Department of Physics, Tokai University, Hiratsuka, Kanagawa 259-1292, Japan
⁴⁵Department of Physics, University of Tokyo, Bunkyo, Tokyo 113-0033, Japan
⁴⁶Kavli Institute for the Physics and Mathematics of the Universe (WPI), The University of Tokyo Institutes for Advanced Study, University of Tokyo, Kashiwa, Chiba 277-8583, Japan
⁴⁷Department of Physics, Tokyo Institute of Technology, Meguro, Tokyo 152-8551, Japan
⁴⁸Department of Physics, Faculty of Science and Technology, Tokyo University of Science, Noda, Chiba 278-8510, Japan
⁴⁹TRIUMF, 4004 Wesbrook Mall, Vancouver, BC, V6T2A3, Canada
⁵⁰Department of Engineering Physics, Tsinghua University, Beijing, 100084, China
⁵¹Faculty of Physics, University of Warsaw, Warsaw, 02-093, Poland
⁵²Department of Physics, University of Warwick, Coventry, CV4 7AL, UK
⁵³Department of Physics, University of Winnipeg, MB R3J 3L8, Canada
⁵⁴Department of Physics, Yokohama National University, Yokohama, Kanagawa, 240-8501, Japan